

## ORIGINAL ARTICLE

# Circular RNA CirCHIPK3 promotes cell proliferation and invasion of breast cancer by sponging miR-193a/HMGB1/PI3K/AKT axis

Zhen-Gang Chen<sup>1</sup>, Hong-Jie Zhao<sup>1</sup>, Ling Lin<sup>1</sup>, Jin-Bo Liu<sup>1</sup>, Jing-Zhen Bai<sup>2</sup> & Guang-Shun Wang<sup>1</sup> <sup>1</sup> Department of Oncology, Tianjin Baodi Hospital, Baodi Clinical College of Tianjin Medical University, Tianjin, China<sup>2</sup> Department of General Surgery, Tianjin Baodi Hospital, Baodi Clinical College of Tianjin Medical University, Tianjin, China**Keywords**

Breast cancer; CirCHIPK3; endogenous competitive RNA; miR-193a; high-mobility group box-1.

**Correspondence**Jing-Zhen Bai, Department of General Surgery, Tianjin Baodi Hospital, Baodi Clinical College of Tianjin Medical University, No. 8 Guangchuan road, Baodi District, Tianjin 301800, China.  
Tel: +86-022-29262019  
Fax: +86-022-29262023  
Email: tjsbdqrmmybjz@126.comGuang-Shun Wang, Department of Oncology, Tianjin Baodi Hospital, Baodi Clinical College of Tianjin Medical University, No. 8 Guangchuan road, Baodi District, Tianjin 301800, China.  
Tel: +86-022-29262022  
Fax: +86-022-29262023  
Email: tjsbdqrmmywgs@126.comReceived: 8 April 2020;  
Accepted: 15 July 2020.

doi: 10.1111/1759-7714.13603

Thoracic Cancer **11** (2020) 2660–2671**Abstract****Background:** The aim of this study was to explore the potential mechanism of circular RNA (circRNA) CirCHIPK3 on the malignant proliferation and metastasis of breast cancer (BC).**Methods:** Human BC samples and their matched normal adjacent tissues were obtained from 50 patients to assess the expression of CirCHIPK3 and its relationship with BC prognosis. A series of in vitro and in vivo functional experiments were carried out to elucidate the role of CirCHIPK3 in BC progression and its underlying molecular mechanisms. Moreover, the interaction of CirCHIPK3, miR-193a, and HMGB1 was examined using bioinformatics, FISH, RIP, RNA-pull down and luciferase reporter assays. Western blot analysis was performed to examine the expression of HMGB1, p-PI3K, total PI3K, p-AKT, and AKT after si-CirCHIPK3 transfection.**Results:** Upregulation of CirCHIPK3 was identified in BC, which predicted a worse prognosis in BC patients. Furthermore, it was found that CirCHIPK3 facilitated cell proliferation, migration, and invasion in BC by regulating miR-193a/HMGB1/PI3K/AKT signaling. CirCHIPK3 acted as a sponge for miR-193a to facilitate HMGB1 expression. si-CirCHIPK3 also inhibited tumor growth of BC in nude mice. si-CirCHIPK3 decreased HMGB1/PI3K/AKT signal expression in MDA-MB-231 cells, whereas overexpression of CirCHIPK3 enhanced HMGB1/PI3K/AKT signal.**Conclusions:** CirCHIPK3 regulated miR-193a/HMGB1/PI3K/AKT signaling to facilitate BC development and progression, providing a novel therapeutic target for BC.**Introduction**

Breast cancer (BC) is one of the most common malignant tumors among females, accounting for 7%–10% in all malignancies. BC has become a major disease threatening female health.<sup>1, 2</sup> Although a series of studies have been carried out with regard to various therapies for BC patients, prognosis of some patients still remains poor, and the mortality rate is relatively high, due to tumor metastasis.<sup>3–5</sup> Therefore, investigation of the potential mechanism of migration and invasion of BC and exploring corresponding medical interventions is urgently required.

Circular RNAs (CircRNAs) are a new type of endogenous noncoding RNA (ncRNA), produced by posterior grafting and characterized by a covalent closed-loop free of 3' and 5' ends.<sup>6</sup> CircRNA was first identified in RNA viruses via electron microscopy as early as the 1970s.<sup>7</sup> Unlike linear RNA, circRNA forms a covalently closed loop produced from back-splicing of primary transcripts, conferring on them inherent resistance to exonucleolytic RNA decay.<sup>8</sup> Hence, circRNAs have been typically considered as a byproduct of errant splicing or mRNA process due to low transcript abundance.<sup>9</sup>

CirCHIPK3 (circRNA ID: hsa\_circ\_0000284) is a product of HIPK3 gene's exon 2 splicing and consists of 1099 nucleotides in length.<sup>10</sup> It has been reported that CirCHIPK3 may function through sponging some miRNAs and regulate the progression of various cancers, including gastric,<sup>11</sup> gallbladder and<sup>12</sup> ovarian cancers.<sup>13</sup> However, whether CirCHIPK3 harbors miRNAs with regulatory roles in BC is still unknown.

High-mobility group box-1 (HMGB1), a DNA-binding protein, functions as a cofactor for proper transcriptional regulation in somatic cells.<sup>14</sup> It is also translocated into cytosol and the extracellular space by multiple cellular stressors such as protein aggregate, radiation, oxidation, chemotherapy and intracellular pathogens.<sup>15</sup> During carcinogenesis and cancer therapy, HMGB1 is closely correlated with invasion, metastasis and drug resistance by regulating various signaling pathways of immunity, metabolism, genomic stability, apoptosis and autophagy.<sup>15</sup> It has been reported that both nuclear and cytoplasmic expression of HMGB1 protein in BC were significantly higher than normal breast tissue.<sup>16</sup> In BC patients, a lower expression of HMGB1 was closely associated with worse survival.<sup>16</sup>

In our study, we identified that CirCHIPK3 was upregulated in BC and upregulated CirCHIPK3 levels predict a poor prognosis in BC patients. Moreover, we showed that CirCHIPK3 knockdown suppressed BC cell proliferation, migration, and invasion. Mechanistically, we found that CirCHIPK3 could function as a ceRNA through harboring miR-193a to abolish the suppressive effect on target oncogene HMGB1, which promoted BC growth and metastasis. Therefore, our study for the first time demonstrated the novel role of CirCHIPK3 in BC, and that the CirCHIPK3/miR-193a/HMGB1 signaling pathway might be a promising therapeutic target for BC treatment.

## Methods

### Clinical samples

All tissues were placed immediately in liquid nitrogen after removal from the BC patients and stored at  $-80^{\circ}\text{C}$  until use. All tumors and paired nontumor tissues were confirmed by two experienced pathologists. This study was approved by the Ethics Committee of Tianjin Baodi Hospital, and written informed consent was obtained from all participants prior to sample collection. All procedures performed involving human participants in this study were conducted in accordance with the Declaration of Helsinki and its later amendments or comparable ethical standards.

### Immunohistochemistry (IHC)

IHC was performed as previously described.<sup>17</sup> Ultrasensitive S-P Kit (Maixin-Bio, China) was used. Briefly, sections from

paraffin-embedded tumor tissues from transplanted nude mice were incubated with primary HMGB1 antibodies (Cat No. ab195012, Abcam, Cambridge, UK). Results were evaluated by two pathologists who were blinded to the experiment separately.

### Cell culture

The normal breast cell line MCF-10A and breast cancer cell lines MCF-7, MDA-MB-231, MDA-MB-468 and MDA-MB-453 were purchased from the American Type Culture Collection (ATCC, USA). Cells were incubated in Dulbecco's Modified Eagle's Medium (Invitrogen, USA) or RPMI-1640 medium (Gibco, USA) with the addition of 10% fetal bovine serum (FBS; Gibco, USA) and 1% penicillin and streptomycin. All cells were cultured and incubated in a 5%  $\text{CO}_2$  atmosphere at  $37^{\circ}\text{C}$ .

### Quantitative reverse transcription-polymerase chain reaction (qRT-PCR)

Total RNA in tissues and cells was extracted using the TRIzol method (Invitrogen, Carlsbad,

CA, USA). The extracted RNA was then reverse transcribed into complementary deoxyribose nucleic acid (cDNA) in strict accordance with miScript Reverse Transcription Kit (TaKaRa, Otsu,

Shiga, Japan). The expression levels of CirCHIPK3, miR-193a and HMGB1 were detected via qRT-PCR. Glyceraldehyde 3-phosphate dehydrogenase (GAPDH) and U6 were used as internal references. The relative expression levels of CirCHIPK3, miR-193a and HMGB1 were calculated by the  $2^{-\Delta\Delta\text{Ct}}$  method. The experiment was repeated three times in each group. Primer sequences used in this study were as follows: CirCHIPK3, forward: 5'-TTCAACATATCTACA-ATCTCGGT-3', reverse: 5' ACCATTCACATAGGTCCGT-3'; miR-193a, forward: 5'-TGGGTCTTTGCGGGC-3', reverse: 5'-GAATACCTCGGACCCTGC-3'; U6: forward: 5'-GCTTCGGCAGCACATATACTAAAAT-3', reverse: 5'-CGCTTCAGAATTTGCGTGTGCAT-3'; GAPDH: forward: 5'-CGCTCTCTGCTCCTCCTGTTC-3', reverse: 5'-ATCCGTTGACTCCGACCTTCAC-3'. miR-193a was normalized to U6 while CirCHIPK3 and HMGB1 was normalized to GAPDH.

### Cell transfection

The circular RNA overexpression vector pLCDH-circRNA was purchased from Guangzhou GENESEED Biological Co., Ltd. (Cat. No. GS0104). The sequence of circHIPK3 (CirBase ID: hsa\_circ\_0000284) was obtained from the CirBase database (<http://www.circbase.org/>). The circHIPK3 sequence was amplified and the overexpression

plasmid pLCDH-circHIPK3 was constructed. Circ-CHIPK3 was silenced by specific small interfering RNAs (Circ-CHIPK3 siRNA-sequence: CUACAGGUAUGG CCUCACA) and scramble siRNAs (si-NC) and empty pcDNA3.1 vectors as control (Guangzhou GENESEED Biological Co., Ltd.). The transfection of these plasmids into MDA-MB-231 cells was carried out with Lipofectamine 3000 Reagent (Thermo Fisher Scientific, CA, USA).

### CCK-8 assay

MDA-MB-231 cells in the logarithmic growth phase were harvested. After adjusting the cell density to  $2 \times 10^4$ /mL, the cells were inoculated into a 96-well plate with 100  $\mu$ L cell suspension per well. After that, the 96-well plate was placed in an incubator for further culture. After 24 hours, cell counting kit-8 (CCK-8) (Dojindo, Kumamoto, Japan) was added into each well and cultured in an incubator for a further hour. Then, 96-well plates were placed in a microplate reader to determine the OD value of each well at 450 nm wavelength. The OD values of cells were measured at 24, 48 and 72 hours, respectively, and the proliferation curve plotted.

### Wound healing assay

Wound healing assay was performed to determine the ability of cells to migrate. The transfected MDA-MB-231 cells were placed in a six-well plate, and cultured in a serum-free medium for 24 hours, followed by scratching in parallel with a 200  $\mu$ L pipette and washing free floating cells with PBS. Cell migration was measured at 0 and 24 hours under a light microscope at 100X magnification.

### Transwell invasion assays

The cell migration and invasion assays were conducted using a transwell chamber (Corning, NY, USA), which was coated with (invasion assay) or without (migration assay) the matrigel mix (BD Biosciences, San Jose, CA, USA) according to the manufacturer's protocol. After incubation for 24 hours, the cells located on the upper surfaces of the transwell chambers were scraped with cotton swabs and the cells located on the lower surfaces were fixed with methanol for 10 minutes, followed by staining with crystal violet. The stained cells were then photographed and counted in five randomly selected fields.

### Xenograft tumor formation assay

Nude mice (six-weeks-old) were purchased from the Model Animal Research Center at Nanjing

University (Nanjing, China). All animal experiments were approved by the Animal Care and.

Use Committee of Linyi Hospital and performed based on the Guide for the Care and Use of Laboratory Animals. First,  $4 \times 10^6$  MDA-MB-231 cells with CirCHIPK3 plasmid or negative control were injected into the mammary fat pad of nude mice. The tumor volume was observed every four days. After four weeks, the mice were sacrificed, and the tumors were used for further study.

### RNA immunoprecipitation assay

MDA-MB-231 cells were lysed in complete RNA immunoprecipitation (RIP) lysis buffer supplemented with RNase inhibitor, and the cell extract was incubated with magnetic beads conjugated with anti-Argonaute 2 (AGO2, #ab32381; Abcam) or a control anti-IgG antibody (EMD Millipore) overnight at 4°C. The RNA/antibody complex was washed three times with RIP buffer supplemented with RNase inhibitor and Proteinase K. The RNA was extracted using Trizol (Thermo Fisher Scientific) according to the manufacturer's protocol and was subjected to quantitative reverse transcription polymerase chain reaction (qRT-PCR) analysis.

### Biotin pull-down assay

A pull-down assay with biotinylated RNA was performed as previously described.<sup>18</sup>In brief, for CirCHIPK3 pulled-down miRNAs, the biotinylated-circ HIPK3 probe was incubated with C-1 magnetic beads (Life Technologies, Carlsbad, CA, USA) to generate probe-coated beads, then incubated with sonicated MDA-MB-231 at 4°C overnight, followed by elution and qRT-PCR. For miR-193a pulled-down circ HIPK3, MDA-MB-231 with CirCHIPK3 over-expression were transfected with biotinylated miR-193a mimics or mutant using Lipofectamine 2000. The cells were harvested, lysed, sonicated, and incubated with C-1 magnetic beads (Life Technologies, Carlsbad, CA, USA), eluted with wash buffer and analyzed with qRT-PCR.

### RNA fluorescence in situ hybridization (FISH)

RNA fluorescence in situ hybridization (FISH) assay was performed using a fluorescent in situ hybridization kit (RiboBio, Guangzhou, China) according to the manufacturer's guidelines. FITC-labeled CirCHIPK3 probes (green) and Cy3-labeled miR-193a probes (red) (Ribo-Bio, Guangzhou, China) were measured with the FISH kit, followed by visualization with a confocal microscope. FISH was performed in MCF-7 and MDA-MB-231 cell lines.

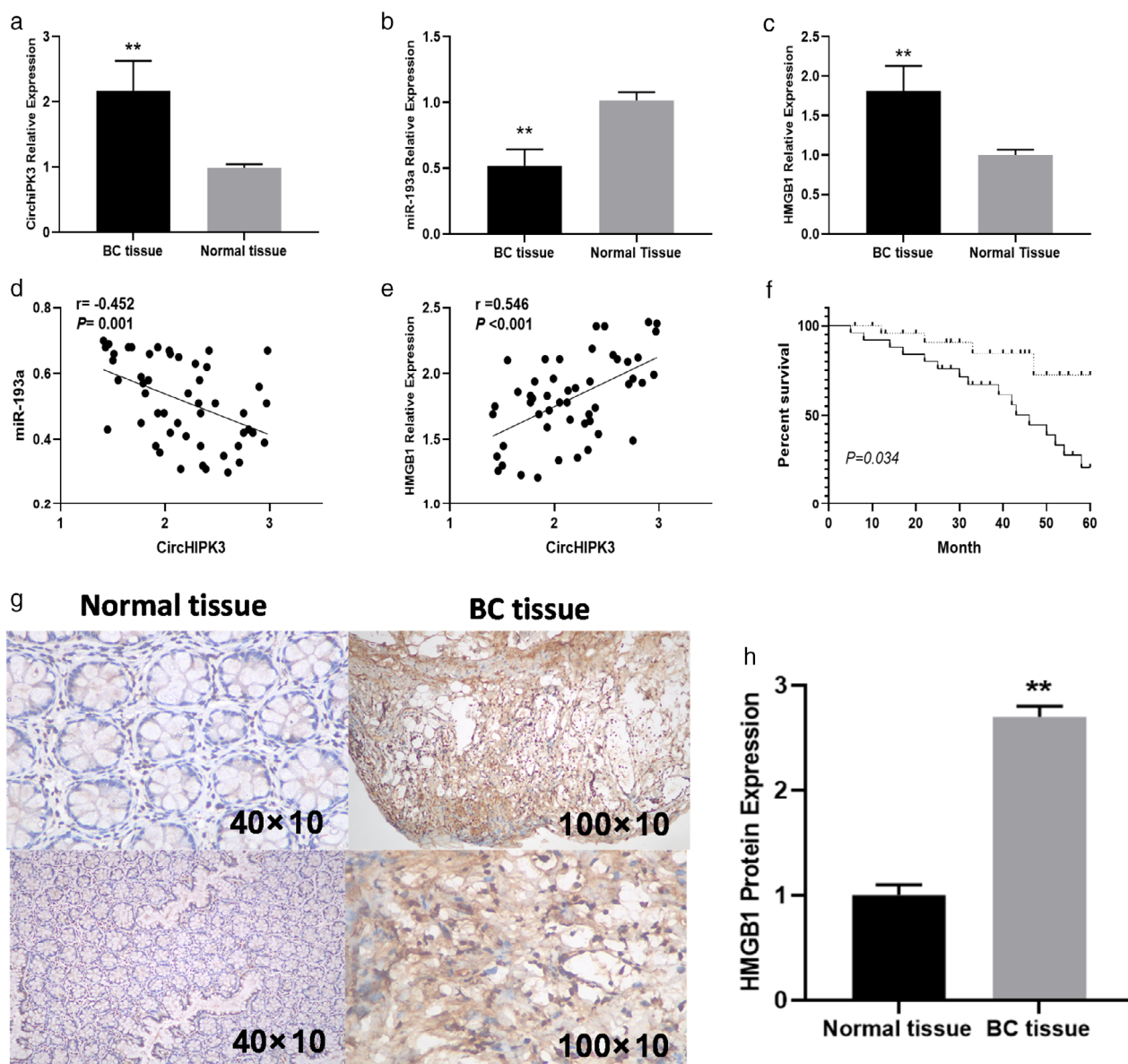


**Figure 1** (a) Comparison of CirCHIPK3 expressions; (b) miR-193a expressions; and (c) HMGB1 expressions between BC tissue and adjacent normal tissue in BC patients. (d) Correlation of miR-193a expressions with CirCHIPK3 expressions in BC tissue. (e) Correlation of HMGB1 expressions with CirCHIPK3 expressions in BC tissue. (f) Kaplan-Meier overall survival curves based on CirCHIPK3 expression levels. (g) HMGB1 expressions detected by IHC between normal tissue and BC tissue. (h) Quantitative analysis of HMGB1 expressions between normal tissue and BC tissue.

### Luciferase reporter assay

The HMGB1 mutant 3'-UTR was generated by replacing the seed regions of the miR-193a binding sites and CirCHIPK3 mutant was generated using site-directed mutagenesis. Subsequently, the mutant sequence was cloned into the firefly luciferase-expressing vector pGL3 (Shanghai GenePharma Co., Ltd). With regard to the luciferase assay, the chondrocytes were seeded in 24-well plates at  $4 \times 10^4$  cells/well the day before transfection and transfected with HMGB1

wild-type or mutant 3'-UTR reporter vector (Shanghai GenePharma Co., Ltd), HMGB1 or HMGB1 mutant using Lipofectamine 2000 (Invitrogen; Thermo Fisher Scientific, Inc). The cells were harvested and lysed 48 hours after transfection and the luciferase activity was assayed using the dual-luciferase reporter system (Promega Corporation, Madison, WI, USA). The  $\beta$ -lactamase gene of the pGL3 luciferase vector was used for the normalization of the luminescence levels. Three independent experiments were performed.

**Table 1** Association of CirCHIPK3 expression with clinicopathological factors of 50 breast cancer patients

Characteristics	CirCHIPK3 expression			P-value
	No.	High (n = 28)	Low (n = 22)	
Age (years)				0.788
≥50	30	16	14	
<50	20	12	8	
Estrogen receptor				0.139
Positive	28	15	13	
Negative	22	13	9	
Tumor size				0.170
≤2 cm	36	18	18	
>2 cm	14	10	4	
TNM stage				0.014*
I-II	34	15	19	
III-IV	16	13	3	
Lymph node metastasis				0.001*
No	33	13	20	
Yes	17	15	2	

\**p* < 0.05. TNM, tumor-node-metastasis

**Western blotting assay**

Cells were washed twice with cold PBS and lysed in RIPA buffer and equal amounts of protein lysates (30 μg per treatment in each lane) were loaded onto the 10% SDS-PAGE gels, then transferred onto polyvinylidene difluoride membranes (PVDF; EMD Millipore, Billerica, MA, USA). After the PVDF membranes had been blocked with 5% skim milk for one hour, they were sequentially incubated with primary antibodies, HRP conjugated secondary antibodies, and visualized using an ECL system (Thermo Fisher Scientific). The primary antibodies used in the study are listed below: HMGB1 (Cat No. ab79823, Abcam), PI3K (Cat No. ab32089, Abcam), p-PI3K (Cat No. ab151549, Abcam), AKT (Cat No. CST4691, Cell Signaling Technology, Danvers, MA), p-AKT (Ser473) (Cat No. CST40589, Cell Signaling Technology) and GAPDH (Cat No. CST#5174T, Cell Signaling Technology). Expression of examined proteins were normalized to GAPDH.

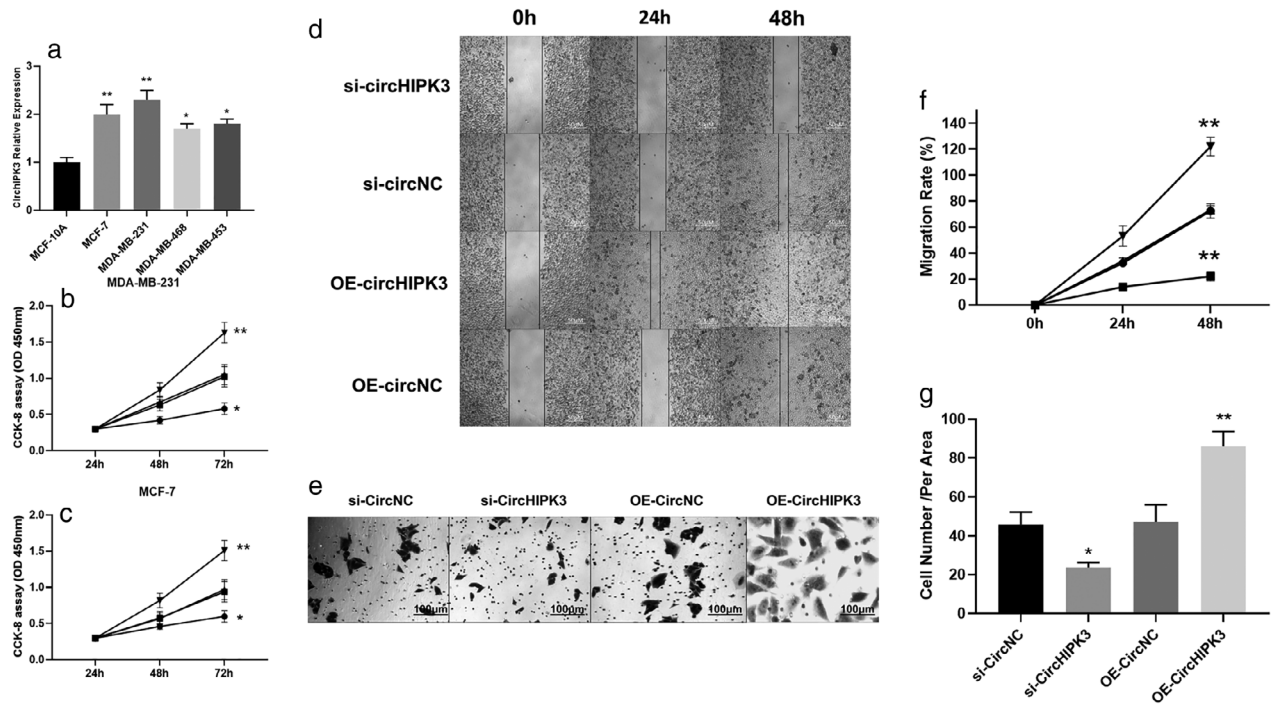


**Figure 2** (a) The expressions of CirCHIPK3 in normal and breast cancer cells. (b) MDA-MB-231 cell proliferation was detected by MTT assay following si-CirCHIPK3 and OE- CirCHIPK3 (\**P* < 0.05, \*\**P* < 0.01) (—●—) si-CirCHIPK3, (—■—) si-CirCNC, (—▲—) OE-CirCNC, (—▼—) OE-CirCHIPK3. (c) MCF-7 cell proliferation was detected by MTT assay following si-CirCHIPK3 and OE-CirCHIPK3 (\**P* < 0.05, \*\**P* < 0.01) (—●—) si-CirCHIPK3, (—■—) si-CirCNC, (—▲—) OE-CirCNC, (—▼—) OE-CirCHIPK3. (d and f) Wound healing assay for migration rate after 0, 24 and 48 hours using MDA-MB-231 cells following si-CirCHIPK3 and OE-CirCHIPK3 (\**P* < 0.05, \*\**P* < 0.01) (—●—) si-CirCHIPK3, (—■—) si-CirCNC, (—▲—) OE-CirCNC, (—▼—) OE-CirCHIPK3. (e and g) Transwell invasion assay for tumor cell invasion after 0, 24 and 48 hours using MDA-MB-231 cells following si-CirCHIPK3 and OE- CirCHIPK3 (\**P* < 0.05, \*\**P* < 0.01).

## Statistical analysis

Differences of Circular RNA CirCHIPK3 expressions between BC tissues and paired adjacent nontumor tissues were analyzed using Student's *t*-test.  $P < 0.05$  was considered to be statistically significant, and all *P*-values were two-sided. All statistical analyses were performed using SPSS software 22.0 (SPSS Inc., Chicago, IL, USA) and GraphPad Prism 6.0 (GraphPad Software, La Jolla, CA, USA).

## Results

### CirCHIPK3 was upregulated in BC tissues and high CirCHIPK3 predicted poor prognosis

First, the expression level of CirCHIPK3 in BC was analyzed. It was found that CirCHIPK3 was significantly upregulated in cancer tissues compared with adjacent

normal tissues (Fig 1a). We also found miR-193a (Fig 1b) was significantly reduced and HMGB1 (Fig 1c) was markedly increased in BC cancer tissues than in adjacent normal tissues. CirCHIPK3 expression was positively related to HMGB1 expressions (Fig 1e) and negatively associated with miR-193a expression (Fig 1d). To assess the association with clinical characteristics of BC patients and CirCHIPK3 expression, we divided the patients into a high expression group ( $n = 28$ ) and low-expression group ( $n = 22$ ) based on the median level of CirCHIPK3 expression. Table 1 shows that increased CirCHIPK3 expression was found to be positively associated with advanced TNM stages (III–IV stages) ( $P = 0.014$ ) and lymph node metastasis ( $P = 0.001$ ). Kaplan-Meier analyses revealed that the high CirCHIPK3 expression group had poorer survival than the low CirCHIPK3 expression group ( $P = 0.034$ ) (Fig 1f). We next detected HMGB1 expressions using IHC, and we found HMGB1 protein expressions were significantly upregulated in BC tissue compared with normal tissue (Fig 1g,h).

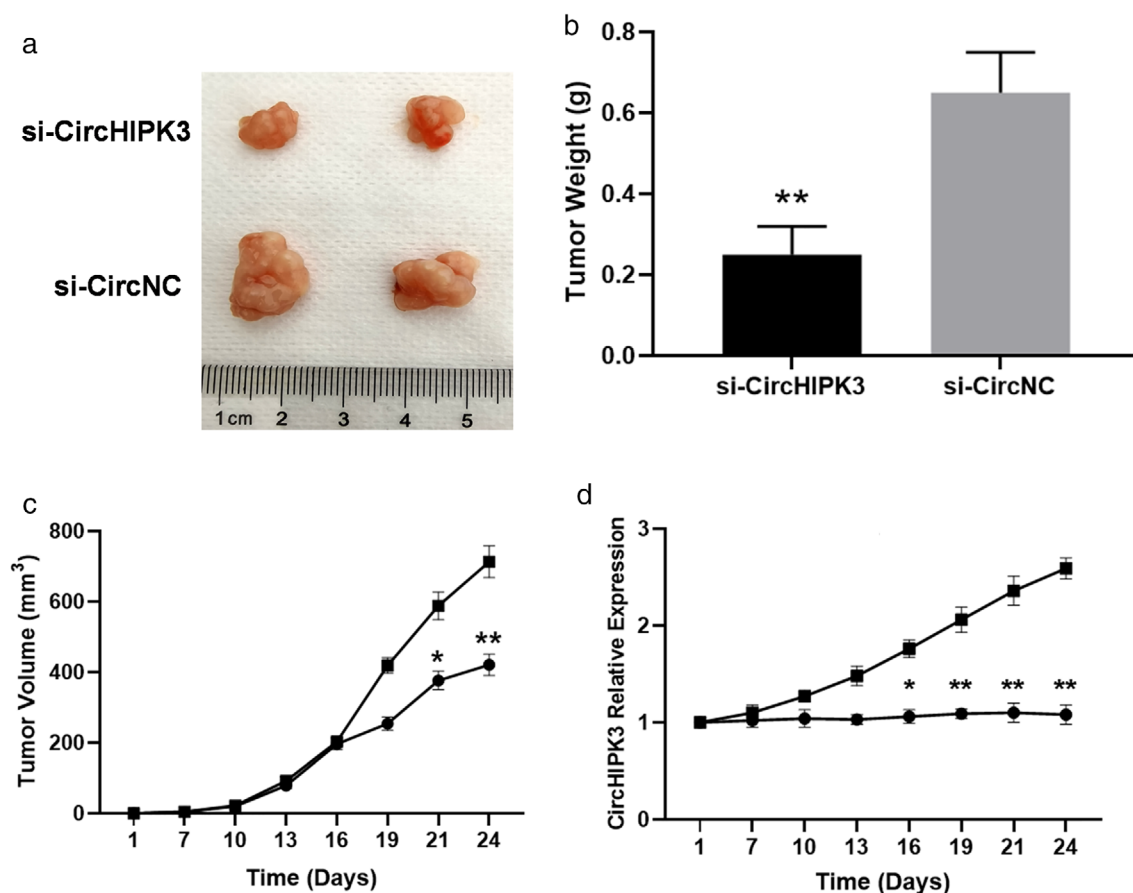


**Figure 3** si-CirCHIPK3 inhibited tumor growth of BC. (a) Representative photographs of BC tumor tissue in si-CirCHIPK3 and si-CircNC groups. (b) Tumor weight in si-CirCHIPK3 and si-CircNC groups at four weeks. \*\* $P < 0.01$ . ( $n = 6$  for each group). (c) Comparison of si-CirCHIPK3 group and si-CircNC group tumor volume from day 1 to day 24 (\*\* $P < 0.01$ , \* $P < 0.05$ ) ( $n = 6$  for each group) (—●—) si-CirCHIPK3, (—■—) si-CircNC. (d) Expressions of CirCHIPK3 during the tumor growth between si-CirCHIPK3 and si-CircNC groups (—●—) si-CirCHIPK3, (—■—) si-CircNC.

### si-CirCHIPK3 decreased BC cell viability, migration, and invasion

Furthermore, similar to the tissue results, CirCHIPK3 expression was significantly upregulated in the BC cancer cell line compared with the normal breast cell line MCF-10A cells (Fig 2a). To further investigate the association between CirCHIPK3 and clinical outcomes, we performed functional assays for cell viability, migration (wound healing assay), and transwell invasion assay in MDA-MB-231 cells (Fig 2b) and MCF-7 cells (Fig 2c). Downregulation of CirCHIPK3 by si-CirCHIPK3 significantly suppressed cell

viability of MDA-MB-231 cells, a cell line that highly expresses CirCHIPK3 (Fig. 2b). In the assessment for functional consequences, downregulation of CirCHIPK3 by si-CirCHIPK3 significantly suppressed the migration (Fig 2d,f) and invasion abilities (Fig 2e,g) of MDA-MB-231 breast cancer cells. In contrast, overexpression of CirCHIPK3 increased BC cell viability, migration, and invasion (Fig 2). Finally, in the xenograft tumor formation assay, we found si-CirCHIPK3 inhibited tumor growth of BC compared with the control at four weeks (Fig 3a-d). Overall, our results revealed that CirCHIPK3 is a tumor suppressive regulator for breast cancer proliferation and metastasis.

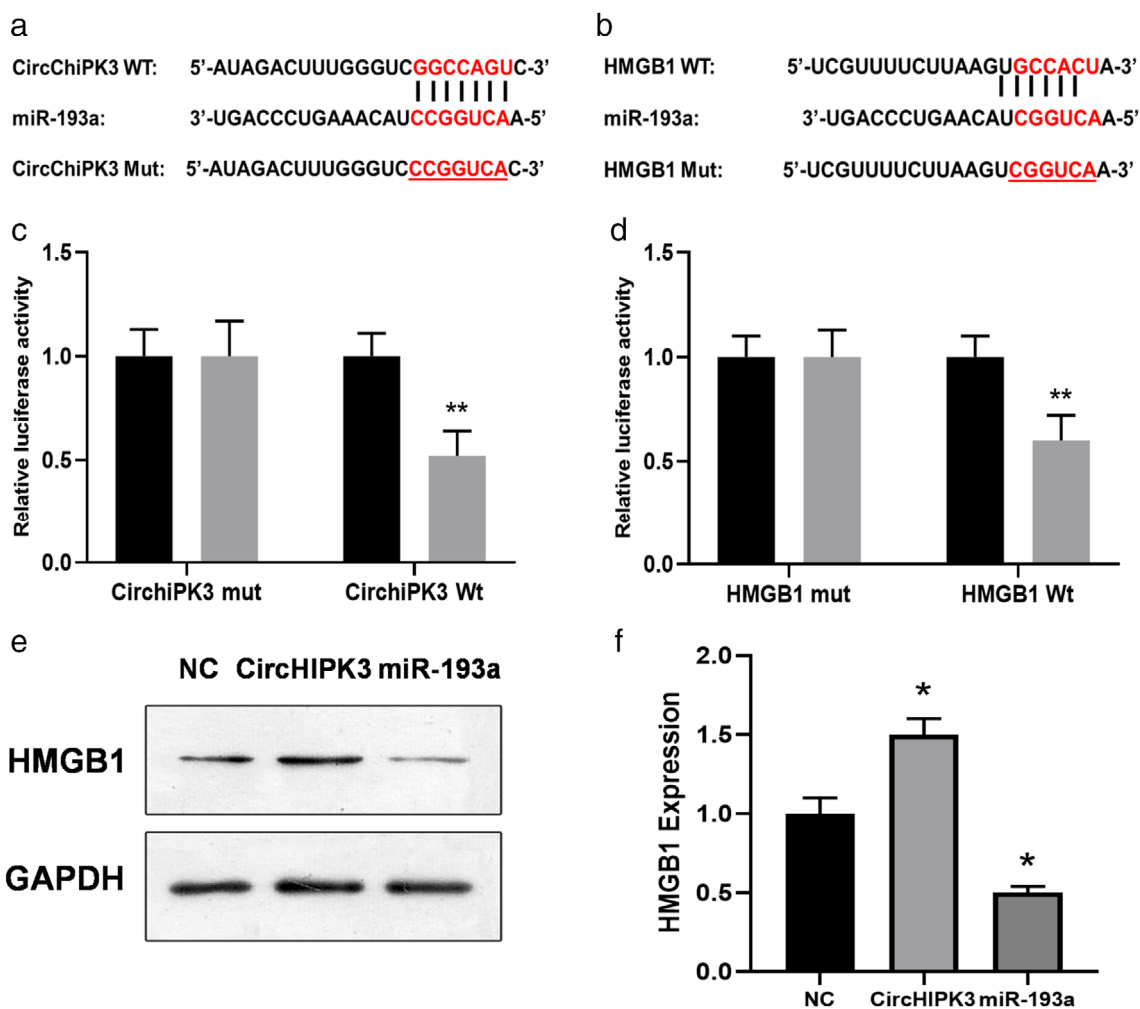


**Figure 4** (a) Bioinformatics analysis of matching sequence of miR-193a within 3'-UTR of CirCHIPK3. Mut CirCPK3 3'-UTR is the mutation of the match sequence of 3'-UTR of CirCPK3 with miR-193a. (b) The predicted binding sites between HMGB1 and miR-193a. Mut HMGB1 3'-UTR is the mutation of the match sequence of 3'-UTR of HMGB1 with miR-193a. (c) Luciferase reporter assay revealed that miR-193a binds to the 3'-UTR of WT CirCHIPK3, not Mut CirCHIPK3 (■) miR-NC, (▨) miR-193a mimic. (d) Luciferase activity was measured in MDA-MB-231 cells cotransfected with mimic NC or miR-193a mimic and HMGB1-wt or HMGB1-mut reporter at 48 hours after transfection (■) miR-NC, (▨) miR-193a mimic. HMGB1 was directly targeted by miR-193a. Relative luciferase activity was quantified and the data were presented as mean  $\pm$  SD (\*  $P < 0.05$ , \*\*  $P < 0.01$ ). (e) Representative images of western blot analysis of CirCHIPK3 and miR-193a on HMGB1 expressions. (f) Quantitative analysis of HMGB1 expressions influenced by CirCHIPK3 and miR-193a mimics (\*  $P < 0.05$ ).

### CirCHIPK3 abolishes the interaction of miR-193a with the targets of HMGB1

We performed bioinformatic analysis to predict the potential target miRNAs in BC, and focused on miR-193a. The predicted complementary binding sites at the 3'-UTR of CirCHIPK3 and HMGB1 are shown in Fig 4a and b, respectively. Bioinformatic analysis also showed that CirCHIPK3 and HMGB1 were potential target genes of miR-193a (Fig 4a,b). Luciferase activity assay showed that miR-193a mimic led to a notable decrease in luciferase activity in CirCHIPK3-WT (Fig 4c) and HMGB1-WT (Fig 4d) reporter compared with the mimic NC group, whereas had no obvious effect on luciferase activity in CirCHIPK3-MUT reporter (Fig 4c). We further carried out western blot analysis to identify whether CirCHIPK3 and

miR-193a mimic could affect HMGB1 expression. We found HMGB1 protein expression was upregulated by CirCHIPK3 and downregulated by miR-193a mimic (Fig 4e,f). In order to further identify the interaction among CirCHIPK3, miR-193a, and HMGB1 in MDA-MB-231 cells, we next carried out RNA pull-down, RIP and FISH assays. RIP assays revealed that CirCHIPK3 and miR-193a expressions were substantially enriched by Ago2 antibody compared with control IgG antibody (Fig 5a). A biotin-coupled probe pull-down assay was then performed and the results showed miR-193a was detected in the CirCHIPK3 pulled-down pellet compared with the control group (Fig 5b). Also, CirCHIPK3 was detected in the miR-193a pulled-down pellet compared with the control group (Fig 5c). FISH technology demonstrated that CirCHIPK3 (green fluorescence) and miR-193a (red fluorescence) could be

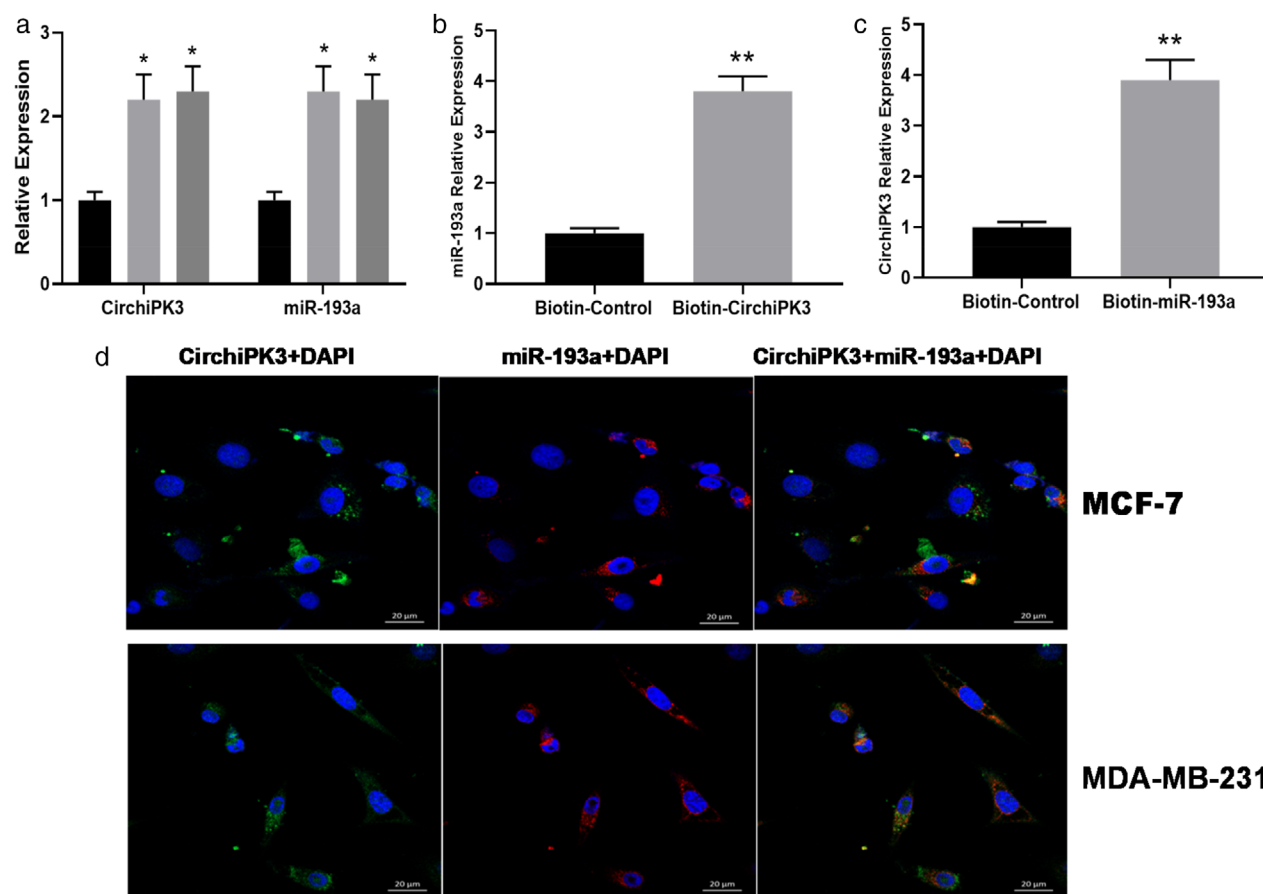


**Figure 5** (a) Relative CirCHIPK3 and miR-193a expression presented as fold enrichment in Ago2 relative to normal IgG immunoprecipitates. RIP assays disclosed that CirCHIPK3 and miR-193a expressions were substantially enriched by Ago2 antibody compared with control IgG antibody (■) Anti-IgG, (▨) Anti-AGO2, (▩) Input. (b) The biotin-coupled probe pull-down assay was performed and the results showed miR-193a was detected in the CirCHIPK3 pulled-down pellet compared with the control group. (c) CirCHIPK3 was detected in the biotin-miR-193a vector compared with the control group. (d) CIRCHIPK3 and miR-193a were colocalized MCF-7 and MDA-MB-231 cells by FISH using confocal microscopy. CirCHIPK3 was stained green, miR-193a was stained red, nuclei were stained blue (DAPI) and overlapped expression was mixed (Scale bar, 20  $\mu$ m). \* $P < 0.05$ , \*\*  $P < 0.01$ .

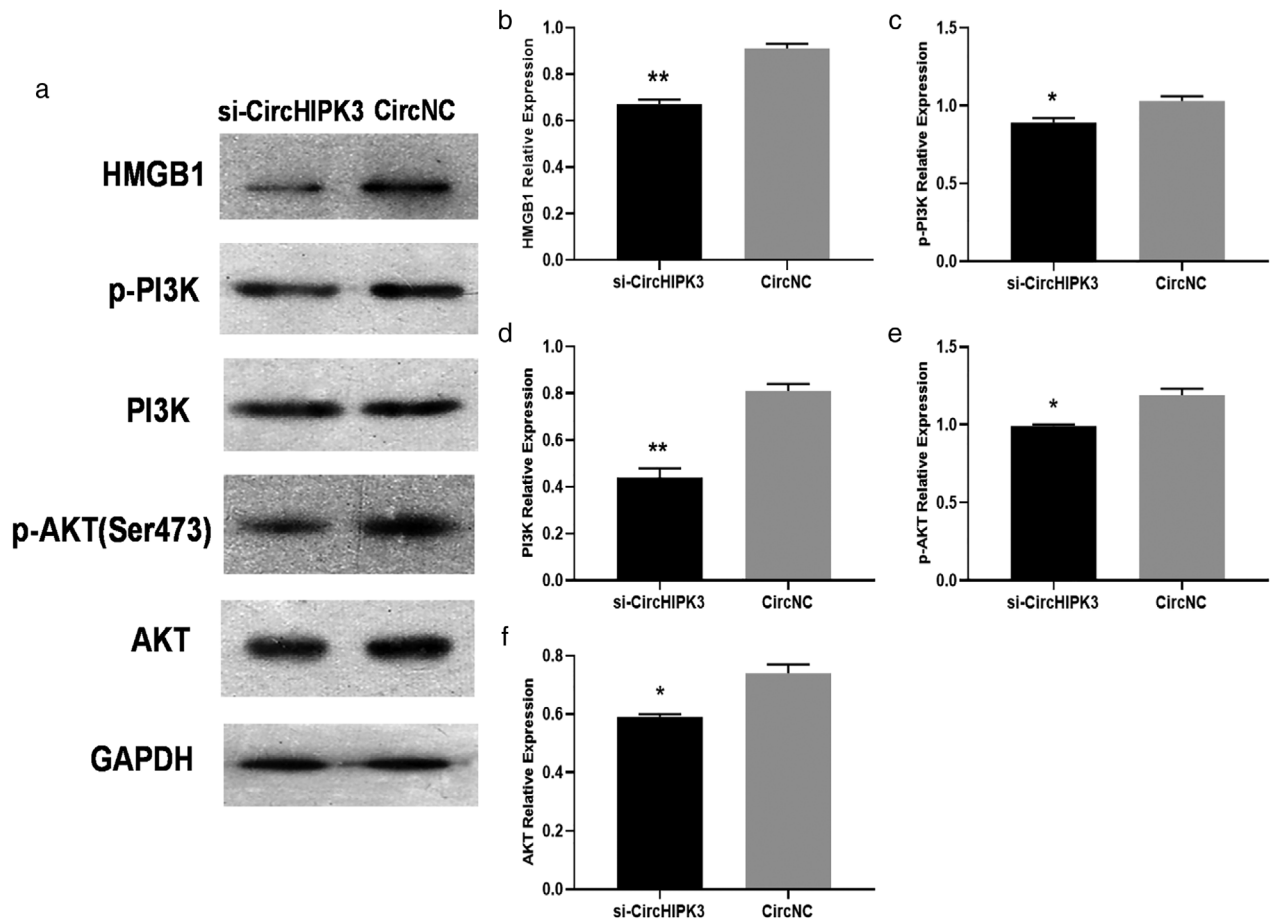


**Figure 6** si-CircCHIPK3 attenuated the HMGB1/PI3K/AKT signaling axis in MDA-MB-231 cells. (a–f) Representative immunoblots (a); quantitative evaluation of HMGB1 (b); PI3K phosphorylation (c); total p-PI3K (d); AKT phosphorylation (e); and total AKT (f) expression in MDA-MB-231 cells subsequent to transient transfection with si-CircCHIPK3 or CircNC. Results are represented as mean  $\pm$  SD. \* $P < 0.05$ , \*\* $P < 0.01$  (compared to vector group).

visualized in the cells, and colocalization was observed in MDA-MB-231 cells (Fig 5d).

### CircCHIPK3 regulated HMGB1/PI3K/AKT signal expression in MDA-MB-231 cells

The PI3K/AKT axis is a crucial participant in tumor metastasis,<sup>19</sup> and a previous study has also shown that HMGB1 could promote angiogenesis and tumor migration via PI3K/AKT signaling.<sup>16</sup> To examine the role of CircCHIPK3 on the HMGB1/PI3K/AKT axis, western blot analysis was carried out, showing that HMGB1, phosphorylated Pi3k and AKT was reduced in MDA-MB-231 cells by transfecting si-CircCHIPK3 compared with CircNC (Fig. 6a–f), whereas these proteins were significantly upregulated by transfecting OE-CircCHIPK3 (Fig. 7a–f). This result suggested that

CircCHIPK3 could regulate HMGB1/PI3K/AKT axis in MDA-MB-231 cells.

### Discussion

Over the past 20 years, circular RNAs have been widely reported and long considered as molecular regulators in various physiological and pathophysiological processes.<sup>20</sup> Recently, due to next-generation sequencing (NGS), numerous circRNAs have been identified from different animal genomes, and many of them were found to be highly stable and abundantly expressed, thereby substantially reshaping the conventional perspective on circRNAs. circRNAs have been reported to be dysregulated in various cancer types. It is widely accepted that these differentially expressed circRNAs may have certain potential functions in the regulation of gene expression.<sup>21</sup> RNA-seq results

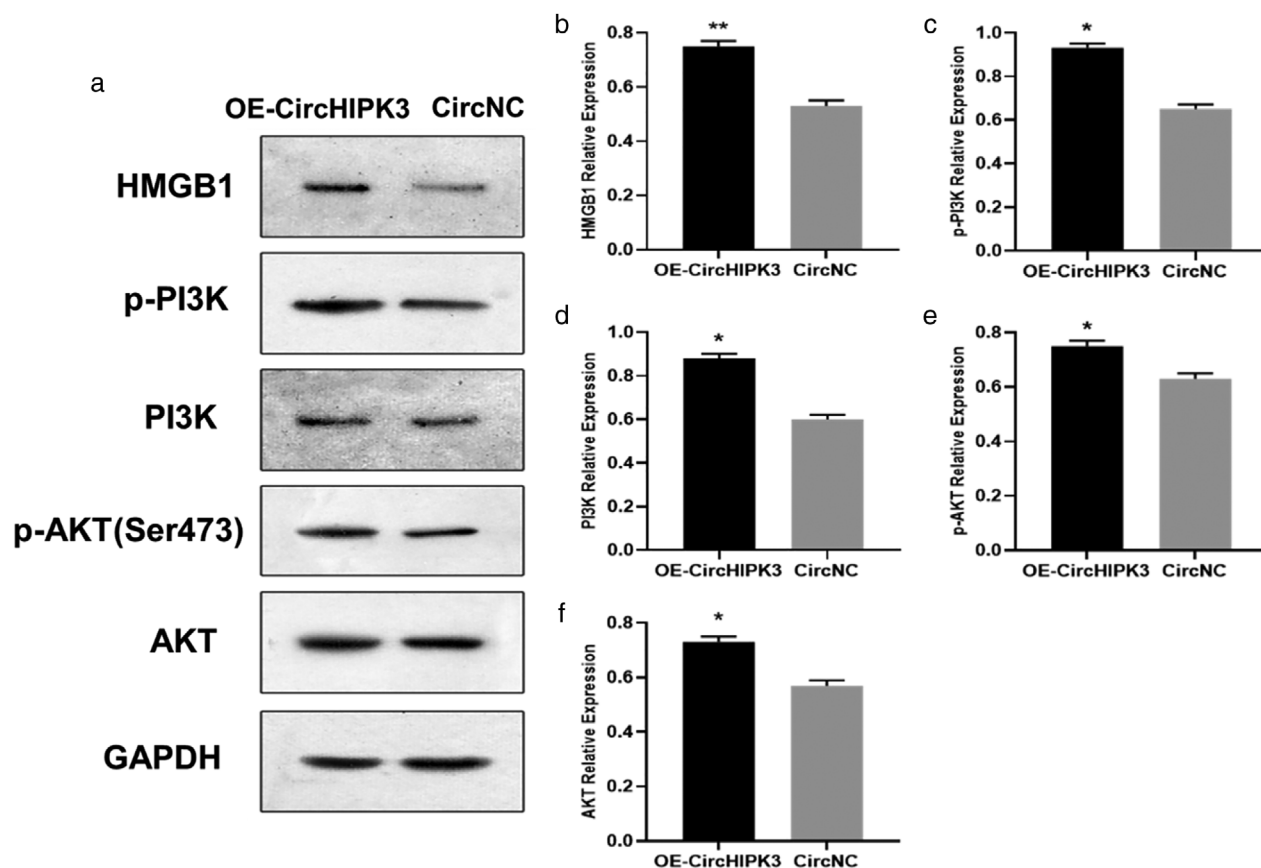


**Figure 7** OE-CircCHIPK3 enhanced the HMGB1/PI3K/AKT signaling axis in MDA-MB-231 cells. (a–f) Representative immunoblots (a); quantitative evaluation of HMGB1 (b); PI3K phosphorylation (c); total p-PI3K (d); AKT phosphorylation (e); and total AKT (f) expression in MDA-MB-231 cells subsequent to transient transfection with OE-CircCHIPK3 or CircNC. Results are represented as mean  $\pm$  SD. \* $P < 0.05$ , \*\* $P < 0.01$  (compared to vector group).

provide useful information for revealing the general tendency of circRNAs expression and assists in the selection of candidate circRNAs for further research.

In the current study, we successfully demonstrated that CirCHIPK3 expression was increased in BC tissues relative to the surrounding nonmalignant tissues. CirCHIPK3 expression was negatively associated with the anticancer gene miR-193a and positively correlated with HMGB1. Moreover, high CirCHIPK3 predicted poor prognosis. This study also revealed that si-CirCHIPK3 decreased the proliferation, migration and invasion capability in BC cells by attenuating HMGB1/PI3K/AKT expression. Hence, our research has proven that CirCHIPK3 has the potential to modulate biological activities in BC via miR-193a/HMGB1, and PI3K/AKT pathway in this process. This research elucidates the effect of CirCHIPK3 on BC etiology and development of therapeutic agents for its treatment.

miR-193a is a member of the miR-193 family. Recent studies have reported the inhibitory effect of miR-193a in a variety of tumors.<sup>22</sup> In 2019, Liu *et al.* found that a low

level of miR-193a-3p expression was related to the increased expression of p21-activated kinase 4 (PAK4), p-Slug, and L1 cell adhesion molecule (L1CAM) in non-small cell lung cancer (NSCLC) and that miR-193a-3p inhibited the metastasis of NSCLC by repressing PAK4, p-Slug, and L1CAM.<sup>23</sup> Through MTT assay and cell colony formation experiments, Yu *et al.* showed that miR-193a-3p was downregulated in colorectal cancer cells, while miR-193a-3p inhibitors promoted the proliferation and invasion of rectal cells.<sup>24</sup> Recently, many researchers have verified that miR-193a-3p acts as an inhibitor in colon, gastric, and breast cancer because it was found to suppress the proliferation, migration, and invasion of these cancer cells.<sup>25–27</sup>

HMGB1, a highly conserved nuclear protein related to chromatin and damage-associated molecular pattern molecule (DAMP) outside the cells, serves as a crucial modulator of apoptosis and cell viability.<sup>28</sup> A previous study has proved that HMGB1 expression is strongly enhanced in BC tissues in comparison with the corresponding surrounding nonmalignant tissues.<sup>29</sup> In addition, high

HMGB1 expression has been reported to be connected to all the hallmarks of malignancy, such as unlimited replicative potential, ability to form vessels, avoiding apoptosis, tolerance towards growth-suppressors, invasion, inflammation, and metastasis.<sup>25</sup>

In our study, we showed CIRCHIPK3 and HMGB1 were both potential target genes of miR-193a through bioinformatic analysis and luciferase activity assay. In addition, CIRCHIPK3 and miR-193a were colocalized MCF-7 and MDA-MB-231 cells by FISH using confocal microscopy, as well as in RIP and RNA pull-down analysis. These results indicated CirCHIPK3 acts as a sponge for miR-193a to facilitate HMGB1 expression in BC cancer cells.

Activation of the PI3K/AKT pathway is a common event in human cancers and is responsible for key aspects of the transformed phenotype.<sup>30</sup> This pathway is activated in most breast cancers via different mechanisms including HER2 amplification, PI3K mutation and PTEN inactivation.<sup>31</sup> In a previous study, HMGB1 has been proven to be a regulator of PI3K/AKT in BC progression.<sup>29</sup> In our study, we found si-CirCHIPK3 inhibited HMGB1 and PI3K/AKT signaling indicating CirCHIPK3 could inhibit BC progression through regulating HMGB1/PI3K/AKT axis.

In conclusion, in this study we show that CirCHIPK3 is upregulated in human BC cancer, and can efficiently sponge miR-193a to increase HMGB1 expression. We also demonstrate that overexpression of CirCHIPK3 can effectively promote aggressiveness and metastasis of BC cells through targeting miR-193a/HMGB1 axis. Our findings provide novel evidence that CirCHIPK3 acts as a microRNA sponge and can be used as a new therapeutic target for the treatment of breast cancer.

## References

- Howell A, Anderson AS, Clarke RB *et al*. Risk determination and prevention of breast cancer. *Breast Cancer Res* 2014; **16**: 446.
- Siegel RL, Miller KD, Jema A. Cancer statistics, 2015. *CA Cancer J Clin* 2015; **65**: 5–29.
- Fan L, Goss PE, Strasser-Weippl K. Current status and future projections of breast cancer in Asia. *Breast Care (Basel)* 2015; **10**: 372–8.
- Cardoso F, Castiglione M. Locally recurrent or metastatic breast cancer: ESMO clinical recommendations for diagnosis, treatment and follow-up. *Ann Oncol* 2009; **20** (Suppl 4): 15–8.
- Wang D, Duan L, Tu Z *et al*. The Glasgow prognostic score predicts response to chemotherapy in patients with metastatic breast cancer. *Chemotherapy* 2016; **61**: 217–22.
- Zhang HD, Jiang LH, Sun DW, Hou JC, Ji ZL. CircRNA: A novel type of biomarker for cancer. *Breast Cancer* 2018; **25**: 1–7.
- Sanger HL, Klotz G, Riesner D, Gross HJ, Kleinschmidt AK. Viroids are single-stranded covalently closed circular RNA molecules existing as highly base-paired rod-like structures. *Pro Natl Acad Sci U S A* 1976; **73**: 3852–6.
- Li J, Sun D, Pu W, Wang J, Peng Y. Circular RNAs in cancer: Biogenesis, function, and clinical significance. *Trends Cancer* 2020; **6**: 319–36.
- Cocquerelle C, Mascrez B, Hetuin D *et al*. Mis-splicing yields circular RNA molecules. *FASEB J* 1993; **7**: 155–60.
- Zheng Q, Bao C, Guo W *et al*. Circular RNA profiling reveals an abundant CirCHIPK3 that regulates cell growth by sponging multiple miRNAs. *Nat Commun* 2016; **7**: 11215.
- Cheng J, Zhuo H, Xu M *et al*. Regulatory network of circRNA-miRNAmRNA contributes to the histological classification and disease progression in gastric cancer. *J Transl Med* 2018; **16**: 216.
- Kai D, Yannian L, Yitian C, Dinghao G, Xin Z, Wu J. Circular RNA HIPK3 promotes gallbladder cancer cell growth by sponging microRNA-124. *Biochem Biophys Res Commun* 2018; **503**: 863–9.
- Liu N, Zhang J, Zhang LY, Wang L. CirCHIPK3 is upregulated and predicts a poor prognosis in epithelial ovarian cancer. *Eur Rev Med Pharmacol Sci* 2018; **22**: 3713–8.
- Lotze MT, Tracey KJ. High-mobility group box 1 protein (HMGB1): Nuclear weapon in the immune arsenal. *Nat Rev Immunol* 2005; **5**: 331–42.
- Tang D, Kang R, Zeh HJ 3rd, Lotze MT. High-mobility group box 1 and cancer. *Biochim Biophys Acta* 2010; **1799**: 131–40.
- Wang CQ, Huang BF, Wang Y, Hu GR, Wang Q, Shao JK. Expression of HMGB1 protein in breast cancer and its clinicopathological significance. *Zhonghua Bing Li Xue Za Zhi* 2020; **49**: 57–61.
- Zheng A, Zhang L, Song X, Wang Y, Wei M, Jin F. Clinical implications of a novel prognostic factor AIFM3 in breast cancer patients. *BMC Cancer* 2019; **19**: 451.
- Li Y, Zheng F, Xiao X *et al*. CirCHIPK3 sponges miR-558 to suppress heparanase expression in bladder cancer cells. *EMBO Rep* 2017; **18**: 1646–59.
- Martini M, De Santis MC, Braccini L *et al*. PI3K/AKT signaling pathway and cancer: An updated review. *Ann Med* 2014; **46**: 372–83.
- Li X, Liu CX, Xue W *et al*. Coordinated circRNA biogenesis and function with NF90/NF110 in viral infection. *Mol Cell* 2017; **67**: 214–27.
- Zhou LH, Yang YC, Zhang RY, Wang P, Pang MH, Liang LQ. CircRNA\_0023642 promotes migration and invasion of gastric cancer cells by regulating EMT. *Eur Rev Med Pharmacol Sci* 2018; **22**: 2297–3.
- Mamoori A, Gopalan V, Lam AK. Role of miR-193a in cancer: Complexity and factors control the pattern of its expression. *Curr Cancer Drug Targets* 2018; **18**: 618–28.
- Liu X, Min S, Wu N *et al*. miR-193a-3p inhibition of the slug activator PAK4 suppresses non-small cell lung cancer

- aggressiveness via the p53/Slug/L1CAM pathway. *Cancer Lett* 2019; **447**: 56–65.
- 24 Yu HM, Wang C, Yuan Z *et al.* LncRNA NEAT1 promotes the tumorigenesis of colorectal cancer by sponging miR-193a-3p. *Cell Prolif* 2019; **52**: e12526.
- 25 Chou NH, Lo YH, Wang KC *et al.* MiR-193a-5p and -3p play a distinct role in gastric cancer: miR-193a-3p suppresses gastric cancer cell growth by targeting ETS1 and CCND1. *Anticancer Res* 2018; **38**: 3309–18.
- 26 Pekow J, Meckel K, Dougherty U *et al.* miR-193a-3p is a key tumor suppressor in ulcerative colitis-associated colon cancer and promotes carcinogenesis through upregulation of IL17RD. *Clin Cancer Res* 2017; **23**: 5281–91.
- 27 Tsai KW, Leung CM, Lo YH *et al.* Arm selection preference of MicroRNA-193a varies in breast cancer. *Sci Rep* 2016; **6**: 28176.
- 28 Zhu J, Wang FL, Wang HB *et al.* TNF-alpha mRNA is negatively regulated by microRNA-181a-5p in maturation of dendritic cells induced by high mobility group box-1 protein. *Sci Rep* 2017; **7**: 12239.
- 29 He H, Wang X, Chen J, Sun L, Sun H, Xie K. High-mobility group box 1 (HMGB1) promotes angiogenesis and tumor migration by regulating hypoxia-inducible factor 1 (HIF-1 $\alpha$ ) expression via the phosphatidylinositol 3-kinase (PI3K)/AKT signaling pathway in breast cancer cells. *Med Sci Monit* 2019; **25**: 2352–60.
- 30 Huang CY, Chiang SF, Ke TW *et al.* Cytosolic high-mobility group box protein 1 (HMGB1) and/or PD-1+ TILs in the tumor microenvironment may be contributing prognostic biomarkers for patients with locally advanced rectal cancer who have undergone neoadjuvant chemoradiotherapy. *Cancer Immunol Immunother* 2018; **67**: 551–62.
- 31 Saini KS, Loi S, De Azambuja E *et al.* Targeting the PI3K/AKT/mTOR and Raf/MEK/ERK pathways in the treatment of breast cancer. *Cancer Treat Rev* 2013; **39**: 935–46.